issn 0065-3713

INSTITUT D'AERONOMIE SPATIALE DE BELGIQUE

3 - Avenue Circulaire
B - 1180 BRUXELLES

AERONOMICA ACTA

ACTA A N° 376

Reactions of nitric acid with di- and tri-chloride ions, di- and tri-iodide ions and with CO_4^- in the gas phase

by

C. AMELYNCK, D. FUSSEN AND E. ARIJS

BELGISCH INSTITUUT VOOR RUIMTE-AERONOMIE

3 - Ringlaan
B - 1180 BRUSSEL

FOREWORD

This article will be published in the INTERNATIONAL JOURNAL OF MASS SPECTROMETRY AND ION PROCESSES.

VOORWOORD

Dit artikel zal verschijnen in de INTERNATIONAL JOURNAL OF MASS SPECTROMETRY AND ION PROCESSES.

AVANT–PROPOS

Cet article paraîtra dans le INTERNATIONAL JOURNAL OF MASS SPECTROMETRY AND ION PROCESSES.

VORWORT

Dieser Artikel wird im INTERNATIONAL JOURNAL OF MASS SPECTROMETRY AND ION PROCESSES erscheinen.

REACTIONS OF NITRIC ACID WITH DI- AND TRI-CHLORIDE IONS, DI- AND TRI-IODIDE IONS AND WITH CO_4^- IN THE GAS PHASE

C. Amelynck, D. Fussen and E. Arijs
Belgian Institute for Space Aeronomy
Ringlaan, 3
B-1180 Brussels Belgium

Abstract

The ion–molecule reactions of HNO_3 with Cl_n^- and I_n^- ($n = 2,3$) have been studied at room temperature by means of a flow tube coupled to a quadrupole mass spectrometer. The reaction rates for $Cl_n^- + HNO_3$ for n=2 and 3 have been determined relative to the known reaction rate for n=1. Nitric acid reacts with Cl_3^-, resulting mainly in the product ion $NO_3^-.HCl$. The product ion(s) of the slower two body reaction of Cl_2^- could not be determined unambiguously, but from thermodynamical considerations $NO_3^-.HCl$ seems to be the most probable candidate. For the study of $I_n^- + HNO_3$, the known reaction $CO_3^- + HNO_3$ was used as a reference. No reaction has been observed for HNO_3 with I_n^-–ions ($n = 2,3$). Additionally rate constants have been determined for the reactions of nitric acid with CO_4^-, $(NO_3OH)^-$, $(NO_3HO_2)^-$ and $NO_3^-.HCl$.

SAMENVATTING

De ion-molekule reakties van HNO_3 met Cl_n^- en I_n^- (n=2,3) werden bestudeerd bij kamertemperatuur aan de hand van een *flow tube* verbonden met een kwadrupool massaspektrometer. De snelheidskonstanten voor $Cl_n^- + HNO_3$ voor n=2 en 3 werden bepaald relatief ten opzichte van de bekende snelheidskonstante voor n=1. De reaktie van HNO_3 met Cl_3^- resulteert voornamelijk in het produktion $NO_3^-.HCl$. Het produktion van de tragere tweelichaamsreaktie met Cl_2^- konden niet eenduidig worden bepaald, maar uit thermodynamische overwegingen blijkt dat $NO_3^-.HCl$ de meest waarschijnlijke kandidaat is. Voor de studie van $I_n^- + HNO_3$ werd de gekende reaktie $CO_3^- + HNO_3$ als referentie gebruikt. Geen reaktie werd waargenomen voor HNO_3 met I_n^- ionen (n=2,3). Daarnaast werden ook de snelheidskonstanten bepaald van de reakties van salpeterzuur met CO_4^-, $(NO_3OH)^-$, $(NO_3HO_2)^-$ en $NO_3^-.HCl$.

RESUME

Les réactions ion–molécule de HNO_3 avec Cl_n^- et I_n^- (n=2,3) ont été étudiées à température ambiante à l'aide d'un tube à écoulement couplé à un spectromètre de masse quadrupolaire. Les coefficients de réaction de $Cl_n^- + HNO_3$ avec n=2 et 3 ont été déterminés par rapport au coefficient de réaction connu pour n=1. L'acide nitrique réagit avec Cl_3^- en produisant principalement l'ion $NO_3^-.HCl$. L(es) ion(s) produit(s) de la réaction à deux corps plus lente de Cl_2^- n'ont pas pu être déterminés univoquement, mais $NO_3^-.HCl$ semble le candidat le plus probable selon des considérations thermodynamiques. Pour l'étude de $I_n^- + HNO_3$, la réaction connue de $CO_3^- + HNO_3$ a été utilisée comme référence. La réaction de HNO_3 avec des ions I_n^- (n=2,3) n'a pas été observée. Des coefficients de réaction supplémentaires ont été mesurés pour les réactions d'acide nitrique avec CO_4^-, $(NO_3OH)^-$, $(NO_3HO_2)^-$ et $NO_3^-.HCl$.

ZUSAMMENFASSUNG

In einem Strömungsrohr mit angeschlossenem Quadrupol–Massenspektrometer wurden die Ionen–Molekülreaktionen von HNO_3 mit Cl_n^- und I_n^- (=2,3) bei Zimmertemperatur untersucht. Die Reaktionsraten für $Cl_n^- + HNO_3$ für n=2 und 3 konnten mit Hilfe der bekannten Reaktionsrate für n=1 ermittelt werden. Salpetersaüre reagiert mit Cl_3^- und bildet als Produkt–Ion hauptsächlich $NO_3^-.HCl$.
Es war nicht möglich, zweifelsfrei das (die) Produktion(en) der langsameren Zweikörperreaktion von Cl_2^- zu bestimmen; aufgrund thermodynamischer Ueberlegungen ist aber $NO_3^-.HCl$ der warscheinlichste Kandidat.
Bei der Untersuchung der Reaktion $I_n^- + HNO_3$ wurde die bekannte Reaktion $CO_3^- + HNO_3$ als Referenz verwendet. Es wurde keine Reaktion von HNO_3 mit den Ionen I_n^- (n=2,3) beobachtet.
Zusätzliche Reaktionsraten wurden für die Reaktionen von Salpetersaüre mit CO_4^-, $(NO_3OH)^-$, $(NO_3HO_2)^-$ und $NO_3^-.HCl$ ermittelt.

1 Introduction

Recently a new method, *A*ctive *C*hemical *I*onization *M*ass *S*pectrometry (ACIMS), was introduced by Arnold and co-workers [1, 2, 3] for the detection of trace gases in the atmosphere. This technique has hitherto been applied mainly for the derivation of nitric acid vapor concentrations in the stratosphere [4, 5, 6]. Detection of stratospheric HNO_3 by ACIMS is based upon the formation of specific product ions ($CO_3^-.HNO_3$ and $NO_3^-.HNO_3$) from ion–molecule reactions of nitric acid with precursor ions ($CO_3^-(H_2O)_n$ and $NO_3^-(H_2O)_n$). These precursor ions are formed by ionization of stratospheric air in a flow tube, coupled to a balloon borne ion mass spectrometer. The precursor and product ions are guided to the mass spectrometer by an air flow created by a small turbine. From the measurement of the residence time of the ions in the flow tube and the analysis of the relative abundance of the precursor and product ions in the spectra obtained with the mass spectrometer, the mixing ratios of the reactive trace gases can be determined since the rate constants of the ion–molecule reactions involved, have been measured in the laboratory [7].

In a previous paper [8] a modification of the ACIMS method has been described which should allow simultaneous in-situ measurements of the stratospheric HNO_3 and N_2O_5 mixing ratios. The proposed modification consists in the injection of Cl^- and I^- as precursor ions into the flow tube, instead of ionizing the ambient air. If an ion source can be realized, which alternately produces exclusively Cl^- and I^-, only the following ion-molecule reactions with NO_3^- as product ion are thought to occur in the flow tube.

$$Cl^- + HNO_3 \rightarrow NO_3^- + HCl \tag{1}$$

reaction rate coefficient $k_1 = 1.6 \times 10^{-9} cm^3 s^{-1}$

$$Cl^- + N_2O_5 \rightarrow NO_3^- + products \tag{2}$$

reaction rate coefficient $k_2 = 9.4 \times 10^{-10} cm^3 s^{-1}$

$$I^- + HNO_3 \rightarrow NO_3^- + HI \tag{3}$$

reaction rate coefficient $k_3 < 5 \times 10^{-11} cm^3 s^{-1}$ (in fact no reaction has been observed)

$$I^- + N_2O_5 \rightarrow NO_3^- + products \tag{4}$$

reaction rate coefficient $k_4 = 5.9 \times 10^{-10} cm^3 s^{-1}$

Relying upon the kinetics of the ion–molecule reactions 1 to 4 investigated in the laboratory [9, 10], it should be possible to derive the sum of HNO_3 and N_2O_5 concentrations in the case the ion source produces Cl^-–ions and the N_2O_5 concentration when only I^- is injected into the flow tube.
The reactions mentioned above have been used in the laboratory by Viggiano et al. [11] to measure the N_2O_5 concentration in the experimental derivation of the rate constant for the thermal collisional dissociation of dinitrogen pentoxide and to determine the HNO_3 impurity level of N_2O_5 in these experiments.

In order to elaborate the application of the method to stratospheric in–situ measurements, as originally suggested by Böhringer [12], we started the development of new types of balloon borne ion sources for the production of Cl^- and I^- ions. It turns out however that the ion sources practically suitable for balloon borne applications, produce, apart from Cl^- and I^- ions, also cluster halide ions of the type Cl_n^- and I_n^- $(n = 2, 3)$. This is most probably due to the elevated pressure required in the ion source itself which should be kept at a slight overpressure with respect to the already relatively high stratospheric pressure. Although the abundance of the polyhalide ions can be varied by choosing proper source conditions (see experimental section), we were not able to avoid them completely. We therefore found it necessary to study the reactions of those cluster ions with HNO_3 and N_2O_5 in order to allow us to estimate their impact on the proposed method. In this paper rate constant measurements of Cl_n^- and I_n^- ions $(n = 2, 3)$ with HNO_3 are presented.
The detection of the Cl_3^- ion was reported by Melton et al. in 1957 [13], but very little was known about its formation. Later on, Robbiani et al. [14, 15] investigated the formation of Cl_3^- through ion–molecule reactions of Cl^- with sulfuryl chloride. Finally, Babcock and Streit [16] studied the three–body reaction of Cl^- with Cl_2 in He.

The existence of I_3^- ions was already reported in 1928 [17]. Although experimental as well as theoretical work [18] has been done on polyhalide ions, few reactions with Cl_2^- and I_2^- ions and, as far as we know, no reactions with Cl_3^- and I_3^- ions involved have been studied so far.

2 Experimental

The rate constant measurements were performed in a flowing afterglow apparatus of the classical design as developed by the NOAA group [19]. The instrument is schematically represented in figure 1. It consists of a quadrupole mass spectrometer coupled to a cylindrical stainless steel flow tube, with two reactant ion inlet ports and a reactant neutral gas inlet. After injection at one of the two ion inlets, the ions are carried along by a large inert buffer gas flow (Ar) (varying between 500 and 2000 sccm) created by a 500 m^3h^{-1} Roots blower backed by a 120 m^3h^{-1} mechanical rotary pump. At the downstream end of the tube, the majority of the ions are collected by an electrically insulated, positively biased (+ 5 V) plate in which a tiny orifice has been drilled (about 0.03 cm in diameter). Through this orifice a small fraction of the ions can enter the detection chamber, which is pumped by a 1500 l/s cryopump. The current on the inlet plate is measured by a floating electrometer. After entering the detection chamber the ions are focused by a simple electrostatic lens system into the quadrupole, where they are analyzed according to their mass-to-charge ratio. An additional bias voltage can be put onto the quadrupole rods in order to obtain a better transmission. Finally the transmitted ions are detected by a spiraltron electron multiplier producing charge pulses which are transformed into voltage pulses by simple electronics. The latter, after passing a buffer for impedance adjustment, are recorded by a pulse counter. The quadrupole power supply and pulse counter are controlled through an IEEE–488 bus, connected to a workstation running under UNIX.

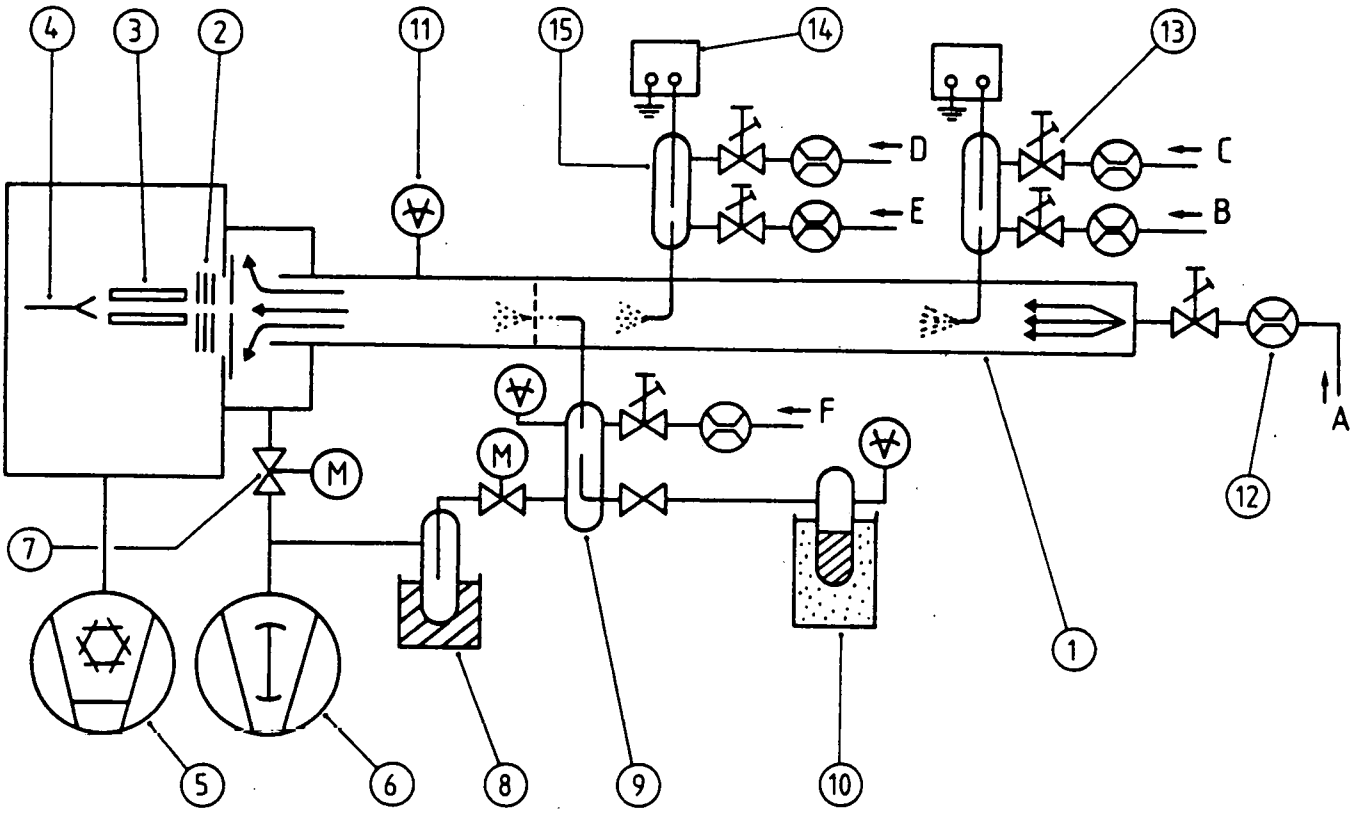

Figure 1:
[A] buffer gas inlet (Ar) [B] ion parent gas mixture inlet (O_2/CO_2) [C] dilution gas inlet (Ar) [D] ion parent gas mixture inlet (Cl_2/Ar or CH_3I/Ar) [E] dilution gas inlet (Ar) [F] dilution gas inlet (Ar) [1] flow tube [2] lens system [3] quadrupole rods [4] Spiraltron detector [5] cryopump [6] Rootspump [7] electronically controlled butterfly valve [8] LN2-trap [9] reactant gas dilution chamber [10] HNO_3–reservoir [11] pressure transducer [12] mass flow meter [13] second ion source [14] ion source power supply [15] first ion source

The two ion sources , respectively situated at a distance of 62 and 86 cm from the sampling aperture, are of a similar design. They consist of a small glass tube in which the ions were produced by a DC gas discharge provoked by a high voltage (1500 V), applied between an electrically insulated needle and the circular entrance of the cylindrical stainless steel tube with an internal diameter of 2 mm. The length of this stainless steel capillary, through which the ions are injected in the flow tube, can be adapted to modify the reactant ion distributions. The ion parent gas and part of the buffer gas (Ar) enter the source through two separate gas inlet ports with MKS–flow meters.

For the production of chlorine ions the source located at 62 cm from the mass spectrometer inlet was used with a high–purity 1000 ppm Cl_2 in Ar mixture as ion parent gas, which

was further diluted with pure Argon. Typical values for the gas flows through the ion source were 10 sccm (standard cubic cm per minute) of the Ar/Cl_2 mixture and 300 sccm noindent of pure Argon. Through these flows and the limited conductance of the steel capillary the pressure in the ion source reaches values of the order of 25 hPa (hectopascal). This value being considerably higher than the pressure in the flow tube (maximum 2.5 hPa), a high speed gas flow emanates in the stainless steel capillary, pushing the ions into the flow tube.

A typical spectrum obtained with the discharge ion source and diluted chlorine is shown in figure 2. As can be seen apart from the masses 35 and 37, due to Cl^-, masses 70, 72 and 74 due to Cl_2^- and masses 105, 107, 109 and 111 due to Cl_3^- are observed.

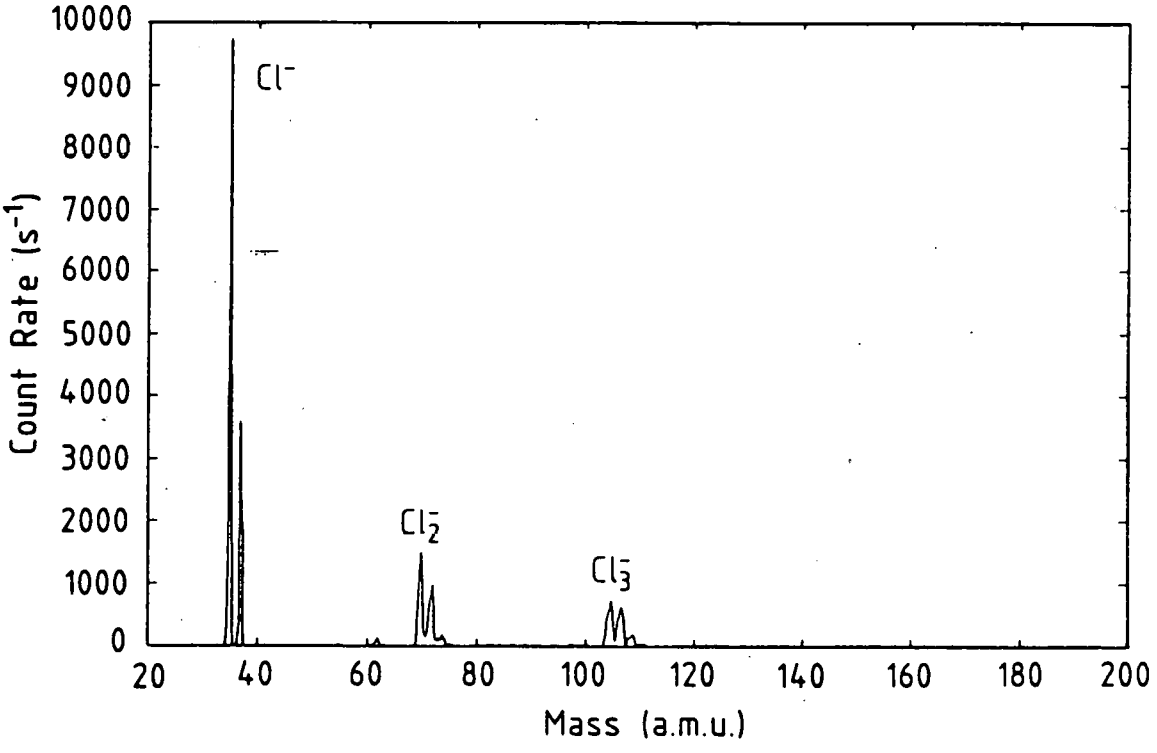

Figure 2: Typical spectrum showing Cl^-, Cl_2^- and Cl_3^- ions produced by sending a mixture of 10 sccm of a 1000 ppm Cl_2 in Ar mixture together with 310 sccm Ar through the first capillary ion source. An additional 450 sccm Ar flow is sent through the flow tube and the flow tube pressure equals 0.66 hPa.

The Cl^- ion is most probably formed by dissociative electron attachment

$$e^- + Cl_2 \rightarrow Cl^- + Cl \tag{5}$$

which was observed in flowing afterglow experiments by Dunkin et al. [20] and which is in agreement with the reported thermal electron attachment coefficient for Cl_2, varying between $2.8 \times 10^{-10} cm^3/s$ and $3.7 \times 10^{-9} cm^3/s$ [21].

As a possible mechanism for the formation of Cl_2^- ions, Lee et al. [22] proposed three-body electron attachment to Cl_2.

$$e^- + Cl_2 + M \rightarrow Cl_2^- + M \tag{6}$$

which has an exothermicity equal to the electron affinity of Cl_2 for which values between 2.3 and 2.6 eV have been found [23,24]. Although the reaction

$$Cl^- + Cl_2 \rightarrow Cl_2^- + Cl \tag{7}$$

is endothermic for about 1.2 eV ($EA(Cl) - EA(Cl_2)$), consistent with the threshold observed by Chupka and Berkowitz [24], it could be a possible formation mechanism for Cl_2^- in the discharge ion source, where the energy of the ions might be larger.

Little, however, is known about the formation of Cl_3^- in the discharge ion source. For the formation of Cl_3^-, Lee et al. suggest the reaction

$$Cl_2^- + Cl_2 \rightarrow Cl_3^- + Cl \tag{8}$$

Taking into account the bond energy $D(Cl_2 - Cl^-)$ of 17 kcalmole^{-1} [15] this reaction is endoergic when the reactants are thermalized. However, at energies $KE_{lab} > 0.3eV$, the reaction has been observed [23] with two pathways:

$$\begin{aligned} Cl_2^- + Cl_2^* &\rightarrow Cl_2^{-*} + Cl_2 && \text{(9a)} \\ &\rightarrow Cl_3^- + Cl && \text{(9b)} \end{aligned}$$

Taking into account the low efficiency (about 0.5 %) of pathway 9b and the high pressure in the ion source, three-body association of Cl^- to Cl_2

$$Cl^- + Cl_2 + M \rightarrow Cl_3^- + M \tag{10}$$

observed with a rate coefficient $k_8 = 9 \times 10^{-30} cm^6/s$ [16] seems to be a more plausible mechanism for the formation of Cl_3^- ions.

For the production of Iodine ions, the same ion source as for Cl_n^- was used but the Ar/Cl_2 gas mixture was replaced by a high-purity mixture of 1000 ppm CH_3I in Ar. Again I_2^- and I_3^- clusters appear next to the I^- ions. The formation of the latter can be understood by

$$e^- + CH_3I \rightarrow I^- + CH_3 \tag{11}$$

for which a value of $7 \times 10^{-8} cm^3/s$ is reported for the electron attachment coefficient [21]. The production of I_n^- ions in an Ar/CH_3I discharge is much harder to understand than the Cl_n^- production in an Ar/Cl_2 discharge. Intuitively it seems rather odd that I_3^- ions would be formed by mere ion-molecule reactions with CH_3I. Most probably formation

of other neutrals (I_2 ?) plays an important role. When using CO_3^- and CO_4^- ions to calibrate the reactions of I_n^- with HNO_3 (see section 3.2) we even had to disable the I_n^- ion source. If we enabled that ion source, the CO_3^- and CO_4^- ions reacted with an unknown neutral, which we could not identify from the product spectrum.

The CO_3^- ions were formed in an O_2/CO_2 discharge, provoked in the ion source located at 86 cm from the mass spectrometer inlet. Apart from the CO_3^- ions, also CO_4^- was formed in the discharge as will be shown in the experimental section. The rate coefficient for the reaction of this ion with nitric acid has also been measured in the experiments reported here.

One of the major dangers in the use of discharge ion sources is the presence of free electrons in the flow tube. Due to the high electron affinity of nitric acid [9], this may give rise to erroneous results in the identification and determination of the relative abundances of the product ions.
The fact that upon addition of nitric acid into the flow tube, the observed ion spectra show no NO_2^-, which in the presence of free electrons would be produced by the very fast reaction

$$e^- + HNO_3 \rightarrow NO_2^- + OH \qquad (12)$$

with $k_{12} = (5 \pm 3) \times 10^{-8} cm^3/sec$ [9] gives strong support for very low free electron concentrations in the flow tube.
Further evidence for the absence of free electrons is given by the measurement of the current versus applied "draw-in" potential on the sampling flange. The current-voltage characteristics which show a negative current for positive draw-in potentials and vice versa indicate the presence of positive ions. A spectrum of the positive source ions from the Ar/CH_3I discharge shows the occurence of several masses between 40 and 140 amu. Taking into account the organic nature of the parent gas (CH_3I), it is difficult to identify the nature of all these species. The most abundant ions had masses 53, 58, 79 and 93. The spectrum of the positive ions from the Ar/Cl_2 discharge was easier to interprete. The most abundant ions were identified as the proton hydrates $H^+.(H_2O)_n$, (n=2,3), Cl_2^+, Cl_3^+, CCl_3^+ and possibly ClO^+ and $COCl^+$.
In any case the symmetrical form of the current-voltage characteristics measured on the draw-in plate (up to the saturation currents) indicates that the concentration of positive ions equals the one of the negative ions in the flow-tube, because a non-negligeable electron concentration in the flow tube should give rise to an important enhancement of the negative saturation current, which was not observed.

The nitric acid reactant gas enters the flow tube axially at a distance of 40 cm from the inlet aperture. The HNO_3-sample was prepared by vacuum-distillation from a HNO_3/H_2SO_4 mixture (volume mixing ratio 1:2) and trapped in a glass reservoir in a cold ethanol bath (-54 $^\circ C$) where it was also stored in the dark. The purity of the HNO_3 was checked by measuring its vapor pressure versus temperature. During measurements the reservoir was held at a constant temperature of 17,5 $^\circ C$ and the HNO_3-vapor was allowed to leak into a stainless steel dilution chamber through a glass capillary, the conductance of which had been calibrated for nitric acid vapor. In this dilution chamber an additional Argon flow was fed and the pressure of the resulting Ar/HNO_3 mixture could

be varied by means of an electronically controlled exhaust valve, connected via a cold trap to the Roots blower. The reactant gas mixture then entered the flow tube through another calibrated glass capillary. From the pressure measurements (vapor pressure of nitric acid and pressure in the dilution chamber), measurement of the Argon flow through the dilution chamber and from the known conductances of the glass capillaries the absolute HNO_3 flow into the flow tube can then in principle be calculated. It turned out, however, that although stable nitric acid flows could be achieved with this method, the reaction rate measurements for reaction 1 were dependent upon the Ar-flow through the dilution chamber. We have attributed this phenomenon to inadequate mixing of HNO_3 and Argon and possible adsorption of nitric acid in the dilution chamber. In view of further difficulties we encountered by applying other methods to realize absolute HNO_3 flows, we decided to perform our measurements in a relative way further on.

In a flow tube experiment the loss of reactant ions is caused by reactions with the reactant gas and by diffusion [19]. In our experimental configuration, the only parameter which is varied for the measurement of the rate coefficient is the rate of addition of the reactant gas (HNO_3). Therefore the loss through diffusion remains constant at the different concentrations of the reactant gas and the simple data analysis as described by Ferguson et al. [19] can be applied. Thus the rate constants for two–body ion–molecule reactions can be obtained by plotting the logarithm of the source ion signal $[X^-]$ versus the reactant concentration $[Y]$ in the flow tube

$$ln[X^-]/[X_o^-] = -k \times \tau \times [Y] \tag{13}$$

where $[X_o^-]$ and τ respectively denote the detected ion concentration with no reactant gas added and the reaction time.
To perform our rate constant measurements in a relative way, we looked at the simultaneous decrease of the $[X^-]$ and $[K^-]$ ion signals where K^- denotes an ion species whose reaction rate constant with HNO_3 is well known. An identical formula holds for the K^- ion.

$$ln[K^-]/[K_o^-] = -k_K \times \tau \times [Y] \tag{14}$$

By simply dividing equation 13 by equation 14 one can infer a value for the unknown coefficient k. The reaction time can easily be measured by the insertion of a grid, immediately behind the reactant gas inlet, allowing to gate the ion signals. Since we only performed relative measurements, the measurement of the ion residence time was irrelevant for the derivation of the reaction rates. Nevertheless it was used in some cases to permit an estimation of the effective HNO_3 concentration in the flow tube.
Since the reactions 1 and

$$CO_3^- + HNO_3 \rightarrow products \tag{15}$$

have been measured before [7, 9], we used Cl^- as K^- to study the reaction of Cl_n^- (n=2,3) ($k_1 = 1.6 \times 10^{-9} cm^3/s$) with HNO_3 and CO_3^- for the reaction of I_n^- (n=2,3) with HNO_3 ($k_{13} = 0.8 \times 10^{-9} cm^3/s$).
As a control for the applied method we derived the rate coefficient of reaction 1 taking

as a reference the well known reaction of CO_3^- with nitric acid [7, 9]. The result of such a check is shown in figure 3 and a value of 2.1 was found for the ratio k_1/k_{15}, which is in excellent agreement with the value found by Fehsenfeld et al. [9].

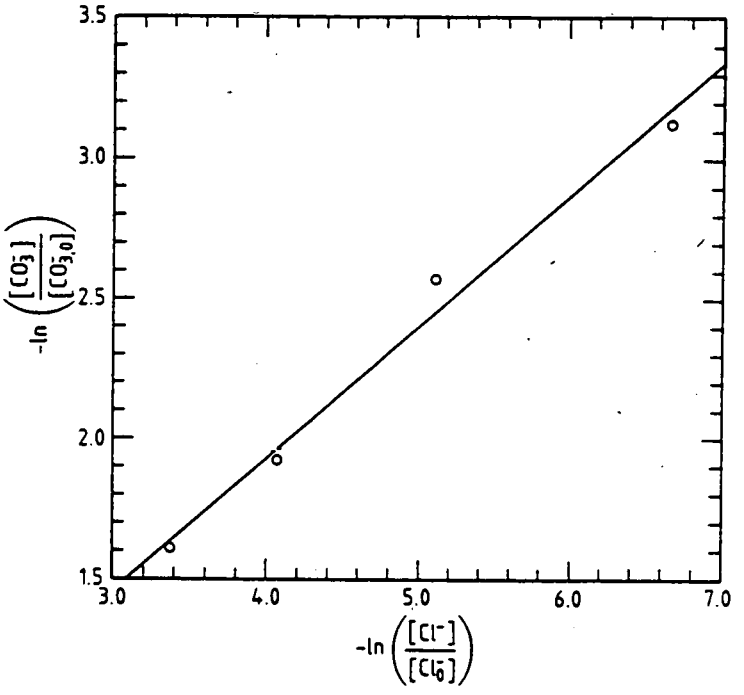

Figure 3: Decay of CO_3^- signal versus Cl^- signal at different HNO_3 densities in the flow tube, leading to a reaction rate constants ratio of 2.1 being in good agreement with the data of Fehsenfeld et al [9]. The Cl^- and CO_3^- ions are respectively created in the first and the second ion source.

3 Results and discussion

3.1 $Cl_n^- + HNO_3$ and further reactions

Figure 4 shows 2 typical spectra obtained, upon addition of nitric acid vapor in the situation where the spectrum of figure 2 was recorded. Whereas the main peaks in figure 2 are clearly attributable to $^{35}Cl^-$ and $^{37}Cl^-$ (natural isotopic abundances 75.8 and 24.2 %), $^{70}Cl_2^-$, $^{72}Cl_2^-$, $^{74}Cl_2^-$, $^{105}Cl_3^-$, $^{107}Cl_3^-$, $^{109}Cl_3^-$ and $^{111}Cl_3^-$, figure 4 shows that upon further addition of HNO_3 the primary Cl_n^- ions disappear while some product ion peaks appear: NO_3^- (mass 62), $NO_3^-.HCl$ (masses 98 and 100), $NO_3^-.HNO_3$ (mass 125) and $NO_3^-.(HNO_3)_2$ (mass 188). From the decay of the signal at mass 35 and 37, the known reaction rate for reaction (1) and the measured time of flight (13 ms) a number density of HNO_3 of about 6×10^{10} molecules/cm^3 and 1.5×10^{11} molecules/cm^3 was found for figure 2A and 2B respectively.

In figure 5 the ion signals of the reactant and product ions are shown as a function of $-ln([Cl^-]/[Cl_o^-])$, which is directly proportional to the HNO_3 concentration in the flow

tube through the relation:

$$[HNO_3] = \frac{-1}{k_1 \times \tau} \times ln\frac{[Cl^-]}{[Cl_o^-]} \tag{16}$$

From figures 4 and 5 it is also clear that NO_3^- is the major product ion of reaction 1, if not the only one.
In order to be able to establish the origin of the $NO_3^-.HCl$ ion, we changed the relative abundances of the reactant ions. To do this, an additional small stainless steel tube (length 10 cm, diameter 0.2 cm) was added between the ion source and the flow tube. As a result, we obtained a situation in which Cl_3^- was the major ion. It is believed that in the longer steel capillary the Cl^- ions are more effectively transformed into Cl_3^- ions by the three–body association reaction 8.

Some typical results as obtained with the ion source with prolonged capillary are shown in figure 6. Here the variation of the ion signals versus the HNO_3 flow is represented for $^{35}Cl^-$, $^{70}Cl_2^-$, $^{105}Cl_3^-$, NO_3^-, $NO_3^-.HCl$, $NO_3^-.HNO_3$ and $NO_3^-.(HNO_3)_2$. In this figure $-ln([^{105}Cl_3^-]/[^{105}Cl_{3,o}^-])$ was taken as a measure for the HNO_3 concentration.

By comparing the relative abundance of the product ion species with the situation where Cl^- was the major peak, we came to the conclusion that $NO_3^-.HCl$ is the major product ion of the reaction of Cl_3^- with HNO_3, most probably through the reaction:

$$Cl_3^- + HNO_3 \rightarrow NO_3^-.HCl + Cl_2 \tag{17}$$

Using the thermochemical data summarized in table 1, it can be easily calculated that reaction 17 is exothermic for an amount of D$(NO_3^-.HCl)$−8.6 kcal/mole, where D$(NO_3^-.HCl)$ is the bond energy of HCl to NO_3^-. It is expected that D$(NO_3^-.HCl)$ is of the order of 20 kcal/mole, considering the bond energy of similar cluster ions, such as $NO_3^-.HNO_3$ and $NO_3^-.HBr$ [25]. No pathways for the reaction of Cl_3^- with HNO_3 leading to NO_3^- and being exothermic could be found.
The reaction product of Cl_2^- with HNO_3 is less evident. Since we were not able to change the ion source conditions in such a way as to make Cl_2^- the most abundant reactant ion, it was impossible to infer the nature of the product ion(s) of Cl_2^- with HNO_3 unambiguously.

The following pathways can be proposed:

$$\begin{aligned} Cl_2^- + HNO_3 &\rightarrow NO_3^- + Cl_2 + H && \text{(18a)} \\ &\rightarrow NO_3^- + HCl + Cl && \text{(18b)} \\ &\rightarrow NO_3^-.HCl + Cl && \text{(18c)} \end{aligned}$$

Reaction 18a is very unlikely, since it is endothermic for about 66 kcalmol^{-1}. From further thermochemical considerations we speculate that the most probable pathway is 18c, since this reaction has an exothermicity of $D(NO_3^-HCl) - 21.2$ kcalmol^{-1}, whereas 18b is endothermic ($\Delta H = 21.2$ kcalmol^{-1}).
Although figure 6 seems to suggest, that the main product of reaction 18 is NO_3^-, because the maximum of the NO_3^- signal is larger than the original Cl^- signal, care must

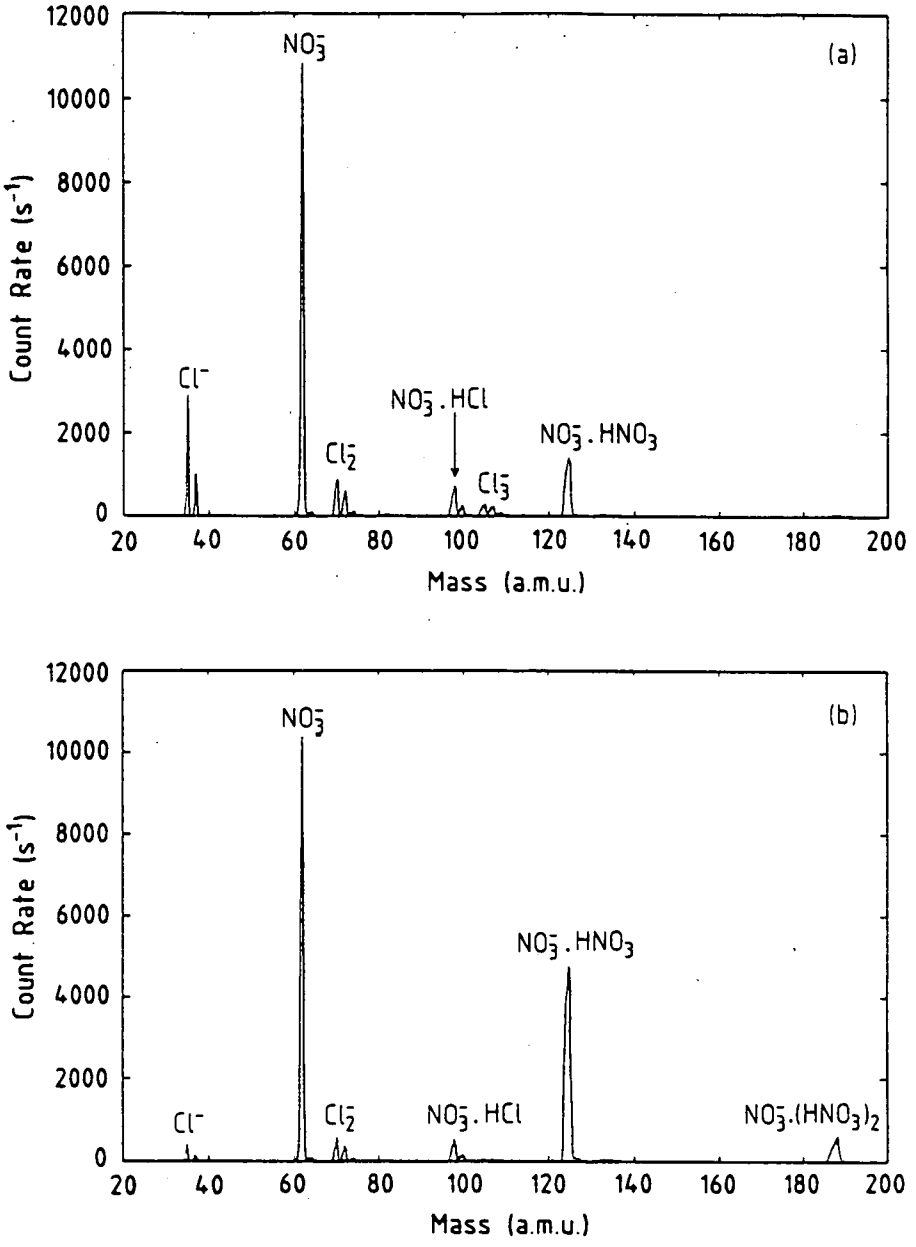

Figure 4:
4a: Spectrum recorded under the same circumstances as in figure 2 but with a nitric acid density in the flow tube of about $6 \times 10^{10} molecules/cm^3$ (as calculated from the decrease of the Cl^- signal). Apart from the three source ions, NO_3^- and $NO_3^-.HCl$ appear as product ions as well as $NO_3^-.HNO_3$, the latter ion species being the result of secondary reactions in the flow tube.
4b: Same conditions as above but with a nitric acid density of about $1.5 \times 10^{11} molecules/cm^3$ in the flow tube. Apart from a further decrease of the Cl_n^- ion signals this picture clearly shows the disappearance of $NO_3^-.HCl$, an increase of the $NO_3^-.HNO_3$ signal and the appearance of $NO_3^-.(HNO_3)_2$ upon further addition of HNO_3.

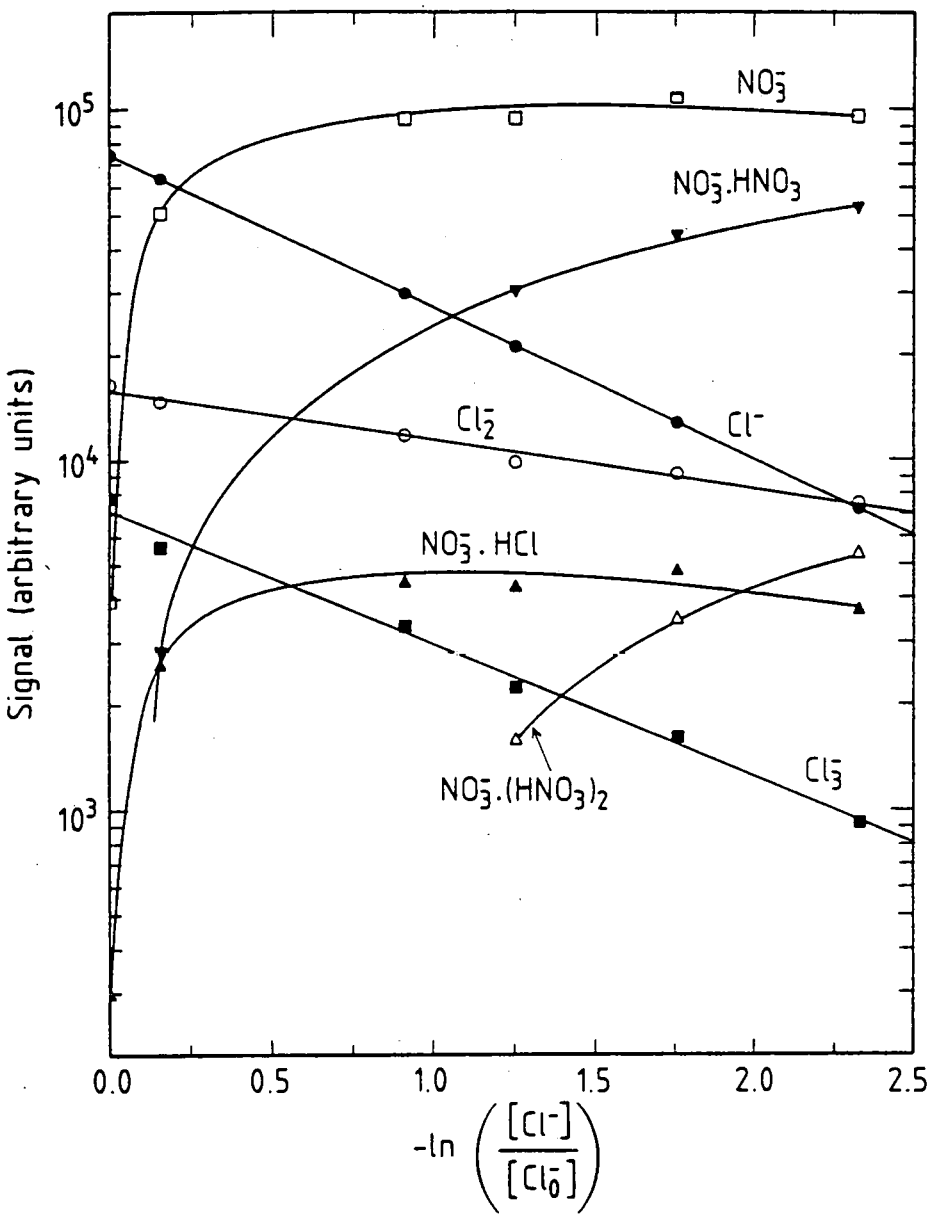

Figure 5: Count rate of the different ions observed in the spectra similar to those of figure 4 as a function of $-ln([Cl^-]/[Cl_o^-])$ (quantity directly proportional to the nitric acid density in the flow tube). The source ions are created in a 200 sccm Cl_2 in Ar (1000 ppm) flow passing through the ion source and the flow tube pressure equals 0.93 hPa. Under these conditions Cl^- clearly is the most abundant source ion and the high NO_3^- count rate confirms that this ion is the product of Cl^- with HNO_3.

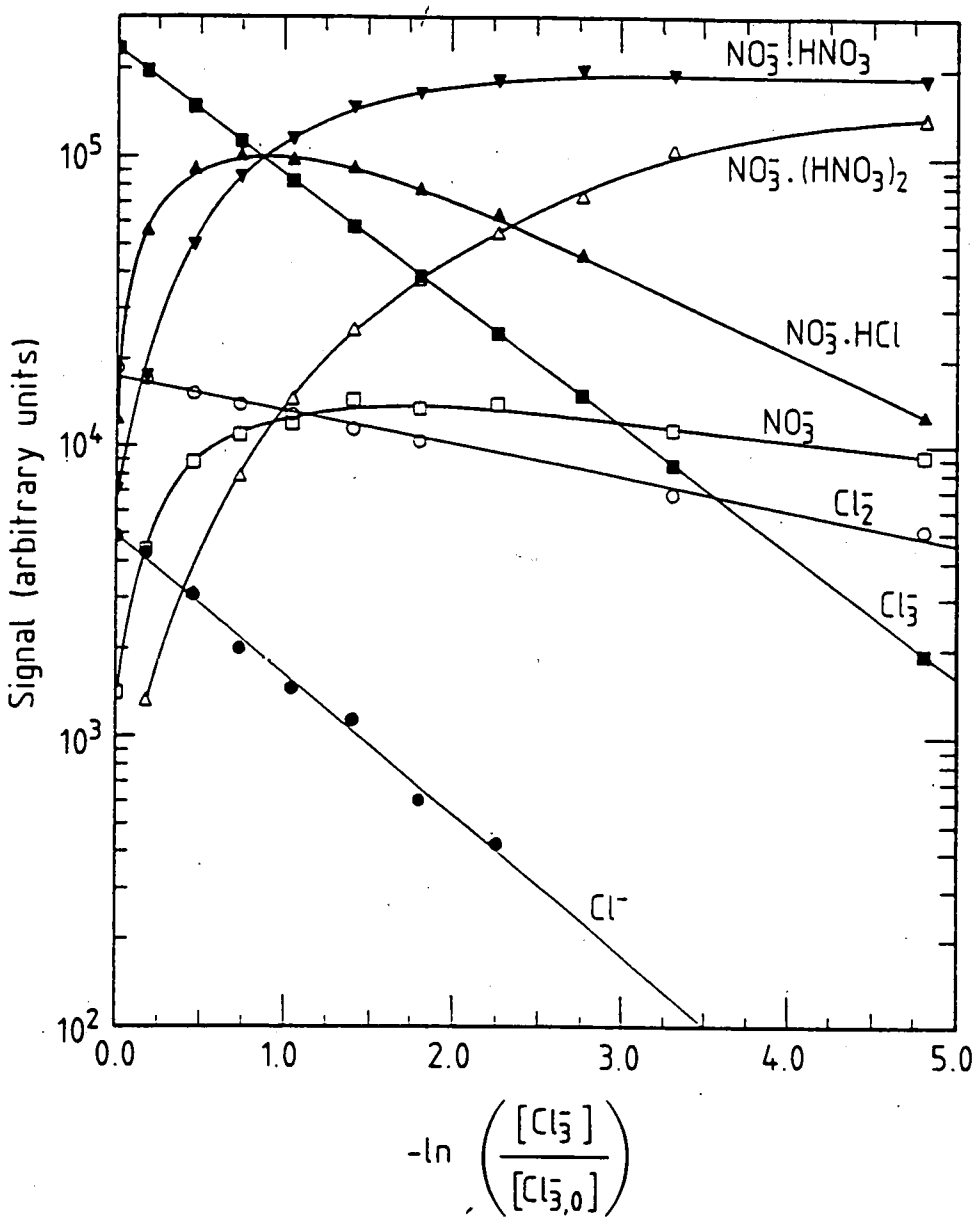

Figure 6: Count rate of the different ions involved versus $-ln([Cl_3^-]/[Cl_{3,o}^-])$ in the situation in which an additional stainless steel tube is added between the ion source and the flow tube in order to make Cl_3^- the most abundant source ion species. An 155 sccm Cl_2 in Ar (1000 ppm) flow is sent through the source. An additional 1800 sccm Ar flow transports the ions towards the spectrometer inlet. Pressure in the flow tube equals 1.14 hPa. The relatively high $NO_3^-.HCl$ ion signal led to the conclusion that this has to be the product of Cl_3^- with HNO_3.

be taken here for different reasons. First it should be kept in mind that NO_3^- could also be produced by thermal decomposition of $NO_3^-.HNO_3$ and $NO_3^-.HCl$, although the contribution of these processes should be small. Second NO_3^- may well be produced in the sampling section of the mass spectrometer itself, due to collision induced dissociation of $NO_3^-.HNO_3$ and $NO_3^-.HCl$ just behind the sampling hole. Finally the detailed interpretation of figure 6 requires a knowledge of the mass discrimination of the detector (mass spectrometer) and the radial diffusion of the different ion species observed. Those data are unfortunately not yet available. (Especially the mass dependent transmission of the quadrupole mass filter can be subtle if its resolution is set by changing the DC to RF ratio as well as by using a programmable ofsett to the DC voltage as was done in our experiments to obtain a more or less constant peak width).
Mass discrimination of the quadrupole and the full detection system can be determined in a SIFT system (Selected Ion Flow Tube) in which one is able to create a situation where the current on the draw–in plate is caused by only one ion species [26]. Since our measurements were not performed in a SIFT and the simultaneous production of different ion species in our discharge ion source in unavoidable, our situation is much more complicated. If we would know the exact distribution of the ions as they enter the flow tube as well as their diffusive behaviour, we could possibly calculate a relative mass discrimination factor for the source ions involved. But finally this wouldn't learn us anything about the mass discrimination for the product ion species.
If reaction 18c is the major loss process for Cl_2^-, then $D(NO_3^-.HCl)$ should be larger than 21.2 kcalmol^{-1}.

From the measurements as those shown in figures 5 and 6 we derived the reaction rate coefficients k_{17} and k_{18} relative to k_1. These values are shown in table 2.

In order to be sure that the reactant ions did not undergo ternary reactions we performed our measurements at different flow tube pressures, ranging from 0.6 to 2.5 hPa (a further increase in flow tube pressure would have led to a deterioration of the vacuum in the detection chamber). The rate constants obtained did not show an explicit pressure dependence, as is shown in figure 7.

Figures 5 and 6 also show that $NO_3^-.HCl$ subsequently disappears upon further addition of nitric acid. Since no other product ions than $NO_3^-.HNO_3$ and $NO_3^-.(HNO_3)_2$ were observed, we concluded that $NO_3^-.HCl$ undergoes the two-body reaction:

$$NO_3^-.HCl + HNO_3 \rightarrow NO_3^-.HNO_3 + HCl \qquad (19)$$

The fact that this reaction takes place implies that $D(NO_3^- HCl)$ is most probably smaller than $D(NO_3^-.HNO_3)$.

The ions NO_3^- and $NO_3^-.HNO_3$ further react with HNO_3 to form respectively $NO_3^-.HNO_3$ and $NO_3^-.(HNO_3)_2$.

$$NO_3^- + HNO_3 + M \rightarrow NO_3^-.HNO_3 + M \qquad (20)$$
$$NO_3^-.HNO_3 + HNO_3 + M \rightarrow NO_3^-.(HNO_3)_2 + M \qquad (21)$$

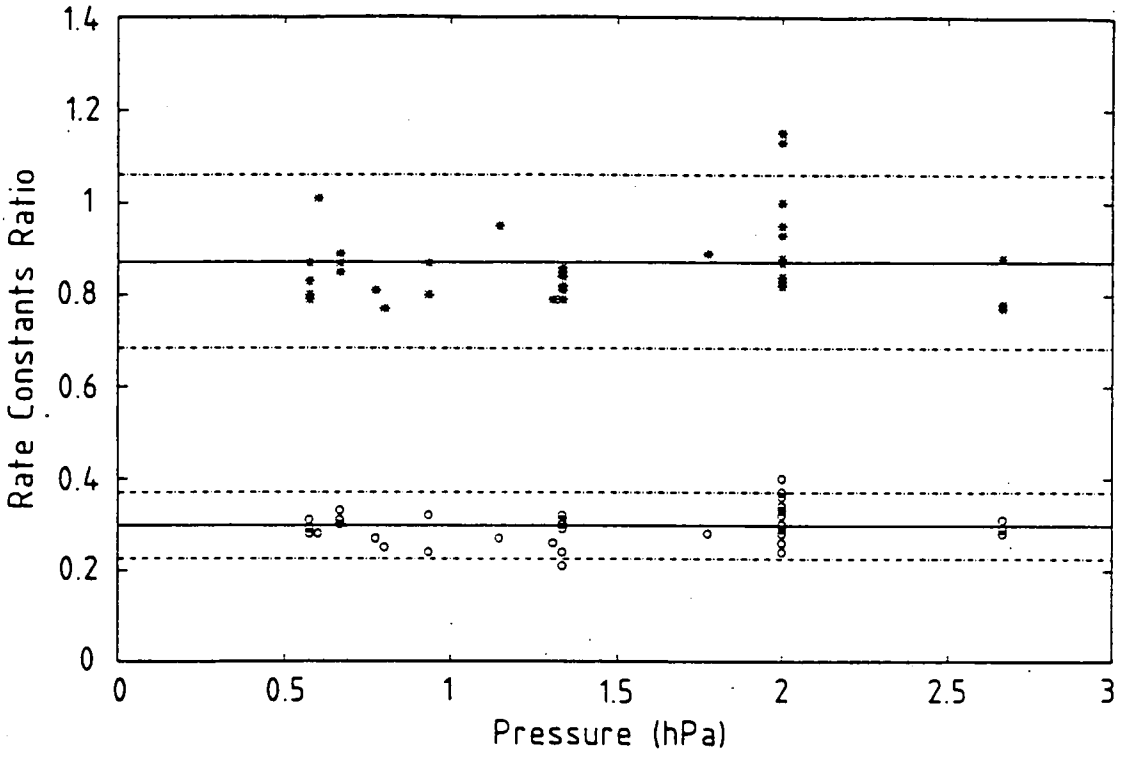

Figure 7: Rate constant ratios for reaction [17] (*) (k_{17}/k_1) and for reaction [18] (°) (k_{18}/k_1) as a function of the flow tube pressure. The full lines represent the mean values. The dashed lines denote a deviation from the mean value of 2σ.

The rate constant of reaction 19 was also measured and is also shown in table 2. The derived value, however, may be subject to a somewhat larger error, and must be considered as a lower limit in view of the possible interference of reaction 18c. The coefficient was derived from the slope of the $NO_3^-.HCl$ signal when the Cl_3^- had already fallen down in order to be sure that little $NO_3^-.HCl$ was produced.
From the linear portions of the NO_3^- signal versus the effective HNO_3 concentrations, a lower limit for the effective two body rate coefficient k_{20} was determined at three different pressures. Considering that only a lower limit is found, the obtained values $3.6 \times 10^{-10} cm^3 s^{-1}, 4.1 \times 10^{-10} cm^3 s^{-1}$ and $5.5 \times 10^{-10} cm^3 s^{-1}$ at respectively 0.93, 1.33 and 2.0 hPa seem to indicate that the clustering is in the high pressure limit of three–body reactions and the value found at 2.00 hPa is even in reasonable agreement with the value $7 \times 10^{-10} cm^3 s^{-1}$ found by Möhler and Arnold [7].

The formation of $NO_3^-.HCl$ by three body association of NO_3^- with HCl has been studied

by A. Viggiano et al. [27]. The $NO_3^-.HCl$ ion was found to be only a minor stratospheric ion by McCrumb and Arnold [28] and Arijs et al. [29]. Reaction 20 and possible similar reactions

$$NO_3^-(HNO_3)_n.HCl + HNO_3 \rightarrow NO_3^-(HNO_3)_{n+1} + HCl \qquad (22)$$

might be responsible for the low abundance of $NO_3^-.HCl$. and $NO_3^-(HNO_3)_n.HCl$ clusters in the stratosphere.

3.2 $I_n^- + HNO_3$ reactions

Fehsenfeld et al. reported an upper limit of only $5 \times 10^{-11} cm^3/s$ for the rate constant of I^- with HNO_3. Since this is a very small value, using this reaction as a reference for the measurement of the rate constants of I_n^- (n=2,3) with HNO_3 is not appropriate. Therefore reaction 15 was chosen as a reference reaction. For these measurements I_n^- ions were produced in the first ion source while CO_3^- ions were made in the second source in an O_2/CO_2 gas mixture. Since the source conditions were such that apart from CO_3^-, CO_4^- ions were produced, we decided to study also the reaction of the latter ion species with HNO_3. The results of this investigation are discussed in the next section.
Typical spectra obtained with the ion source 1 using the CH_3I/Ar mixture are shown in figure 8. Figure 8a shows a spectrum obtained without any reactant gas, whereas figure 8b represents a spectrum upon addition of HNO_3.
The ion signal for $I^-, I_2^-, I_3^-, CO_3^-$ and CO_4^- versus $-ln([CO_3^-]/[CO_{3,o}])$ (a measure for the effective HNO_3 number density in the flow tube) is shown in figure 9. As can be seen the signal of the poly-iodide ions is not decreasing upon further addition of nitric acid. The upper limits for the rate constants of the reactions $I_n^- + HNO_3$ (n=1,2,3), as derived from figure 9 are also represented in table 2.
The only product ion that appeared in very low concentration when increasing the nitric acid flow into the flow tube was $I^-.HNO_3$, probably formed by the following reactions:

$$I^- + HNO_3 + M \rightarrow I^-.HNO_3 + M \qquad (23)$$

$$I_3^- + HNO_3 \rightarrow I^-.HNO_3 + I_2 \qquad (24)$$

When using reaction 15 as a reference for measuring the rate constant of I_n^- with HNO_3 we alternately fed the ion sources so that they didn't work together. This is a very important precaution since in the first ion source an unidentified neutral substance was created together with the iodine ions. This substance reacted with CO_3^- and CO_4^- ions.

3.3 $CO_4^- + HNO_3$ reaction.

A typical spectrum of the reactant ions of the second ion source obtained without reactant neutral gas in the flow tube is shown in figure 10a. The major ion peaks are attributed to CO_3^- (mass 60) and CO_4^- (mass 76). One can also distinguish the apparition of two

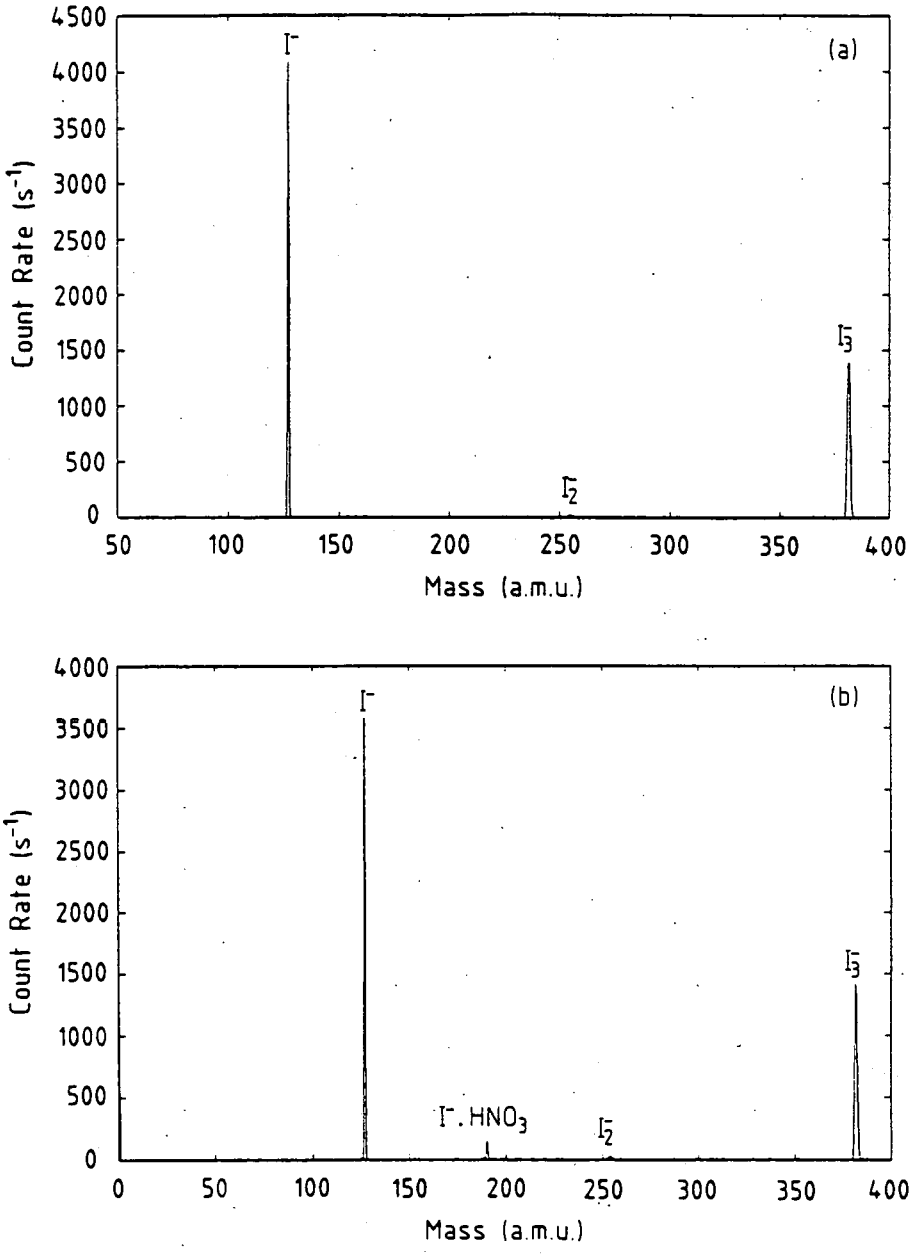

Figure 8:

8a: Spectrum without addition of HNO_3. The I_n^- ions (n=1,2,3) are produced in a 200 sccm CH_3I in Ar (1000 ppm) + 140 sccm Ar gas flow and carried along the flow tube by a 1120 sccm Ar flow. The flow tube pressure equals 0.98 hPa. In this spectrum I_2^- only appears as a minory substance.

8b: Spectrum taken after addition of 29 msccm HNO_3 to the flow tube (as calculated from the measured conductances, flows and pressures related to the HNO_3 dilution system). Note the appearance of a small $I^-.HNO_3$ peak, the origin of which we are not able to determine unambiguously.

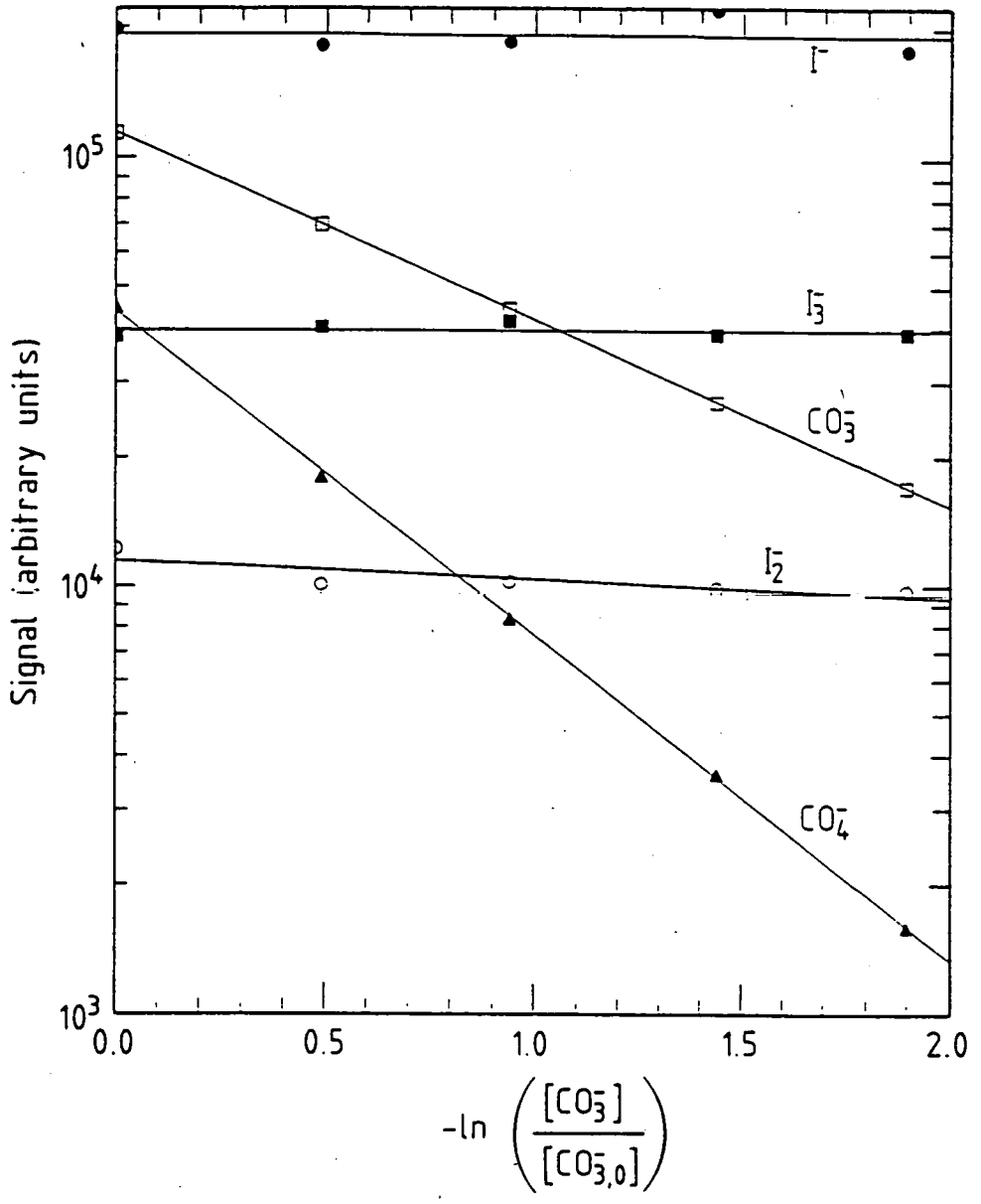

Figure 9: Count rate of I_n^- (n=1,2,3) and CO_k^- (k=3,4) ions versus $-ln([CO_3^-]/[CO_{3,o}^-])$ obtained by using two alternately working ion sources. A 200 sccm CH_3I in Ar (1000 ppm) + 133 sccm Ar flow is sent through the first ion source while a 300 sccm CO_2/O_2 (1:1) mixture is flowing through the second source.

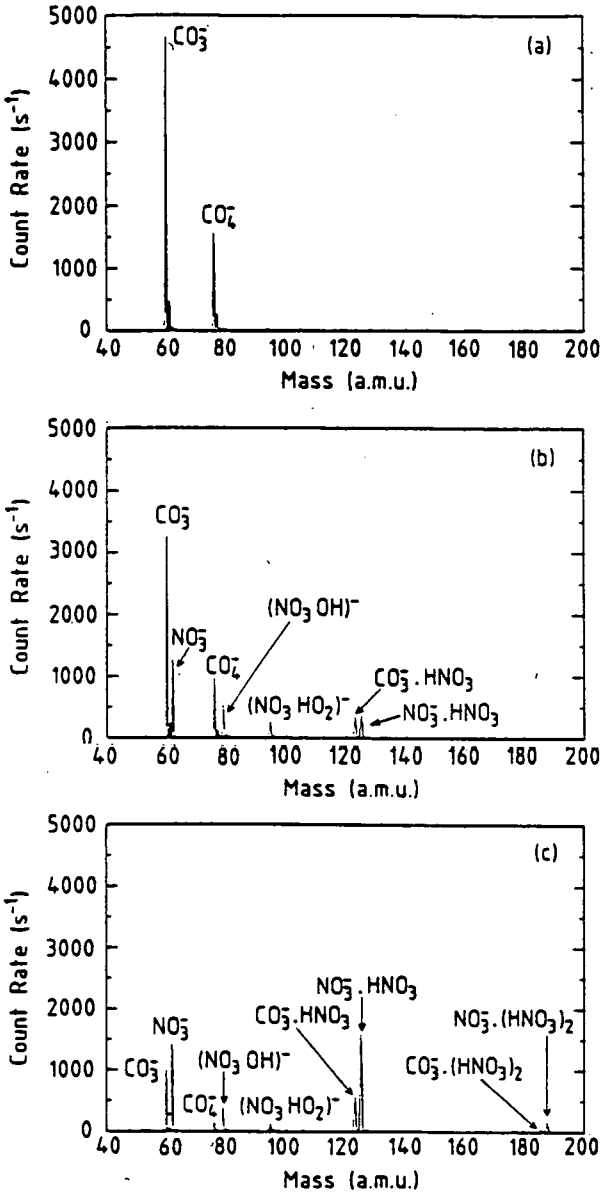

Figure 10:
10a : Spectrum without addition of HNO_3. CO_3^- and CO_4^- are formed in a mixture of 158 sccm CO_2 and 175 sccm O_2 flowing through the second capillary ion source. An 780 sccm inert Ar buffer gas flow is added to the flow tube. The flow tube pressure equals 0.86 hPa. Apart from CO_3^- and CO_4^-, HCO_3^- and HCO_4^- are also present in the spectrum as impurity ion species.
10b: Spectrum taken under the same circumstances as in figure 10a but with a HNO_3 concentration of about $4.5 \times 10^{10} molecules/cm^3$ in the flow tube. Apart from the source ions, NO_3^-, $(NO_3OH)^-$, $(NO_3HO_2)^-$, $CO_3^-.HNO_3$ and $NO_3^-.HNO_3$ can also be seen in this spectrum.
10c: Spectrum with a HNO_3 concentration of about $2 \times 10^{11} molecules/cm^3$ in the flow tube. Remark that, upon further addition of HNO_3, the secondary reaction products $NO_3^-.(HNO_3)_2$ and $CO_3^-.(HNO_3)_2$ also appear.

minor peaks HCO_3^- (mass 61) and HCO_4^- (mass 77). The CO_3^- and CO_4^- ions are thought to be formed in the O_2/CO_2 discharge by the following reaction sequence:

$$\begin{aligned}
e^- + O_2 + M &\rightarrow O_2^- + M && (25a)\\
&\rightarrow O^- + O_3 \quad (M = O_2) && (25b)\\
O_2^- + O_2 + M &\rightarrow O_4^- + M && (26)\\
O_4^- + O &\rightarrow O_3^- + O_2 && (27)\\
O^- + O_2 + M &\rightarrow O_3^- + M && (28)\\
O_3^- + CO_2 &\rightarrow CO_3^- + O_2 && (29)\\
O^- + CO_2 + M &\rightarrow CO_3^- + M && (30)\\
O_2^- + CO_2 + M &\rightarrow CO_4^- + M && (31)\\
O_4^- + CO_2 &\rightarrow CO_4^- + O_2 && (32)\\
CO_3^- + O &\rightarrow O_2^- + CO_2 && (33)\\
CO_4^- + O &\rightarrow CO_3^- + O_2 && (34)
\end{aligned}$$

Upon addition of HNO_3 in the flow tube (figures 10b and 10c) 7 new mass peaks (62, 79, 95, 123, 125, 186 and 188) appear. Masses 62, 79 and 123 can be attributed to NO_3^-, $(NO_3OH)^-$ and $CO_3^-.HNO_3$ respectively and are formed through the reaction of CO_3^- with HNO_3, which according to Möhler and Arnold [7] proceeds via the intermediary complex $[(CO_3.HNO_3)^-]^*$ and has the following pathways:

$$\begin{aligned}
CO_3^- + HNO_3 \rightarrow [(CO_3.HNO_3)^-]^* &\rightarrow NO_3^- + OH + CO_2 && (35a)\\
&\rightarrow CO_3^-.(HNO_3) + M && (35b)\\
&\rightarrow (NO_3OH)^- + CO_2 && (35c)
\end{aligned}$$

The peaks at mass 125 and 188 can be identified as $NO_3^-.HNO_3$ and $NO_3^-.(HNO_3)_2$ clusters, produced by the three body association reactions 18 and 19, whereas the formation of $CO_3^-(HNO_3)_2$ (mass 186) can be explained by the association

$$CO_3^-.HNO_3 + HNO_3 + M \rightarrow CO_3^-.(HNO_3)_2 + M \qquad (36)$$

which was also observed by Möhler and Arnold [7].
The presence of mass 95, which is attributed to $(NO_3HO_2)^-$, suggests that the reaction of CO_4^- with nitric acid has similar pathways as $CO_3^- + HNO_3$, namely

$$\begin{aligned}
CO_4^- + HNO_3 &\rightarrow NO_3^- + products && (37a)\\
&\rightarrow (NO_3HO_2)^- + CO_2 && (37b)
\end{aligned}$$

In figure 11 all major reactant and product ions are plotted versus $-ln([CO_3^-]/[CO_{3,o}^-])$, and thus indirectly versus the nitric acid density in the flow tube. As can be seen from this graph, increasing the nitric acid concentration in the flow tube, results also in the decrease

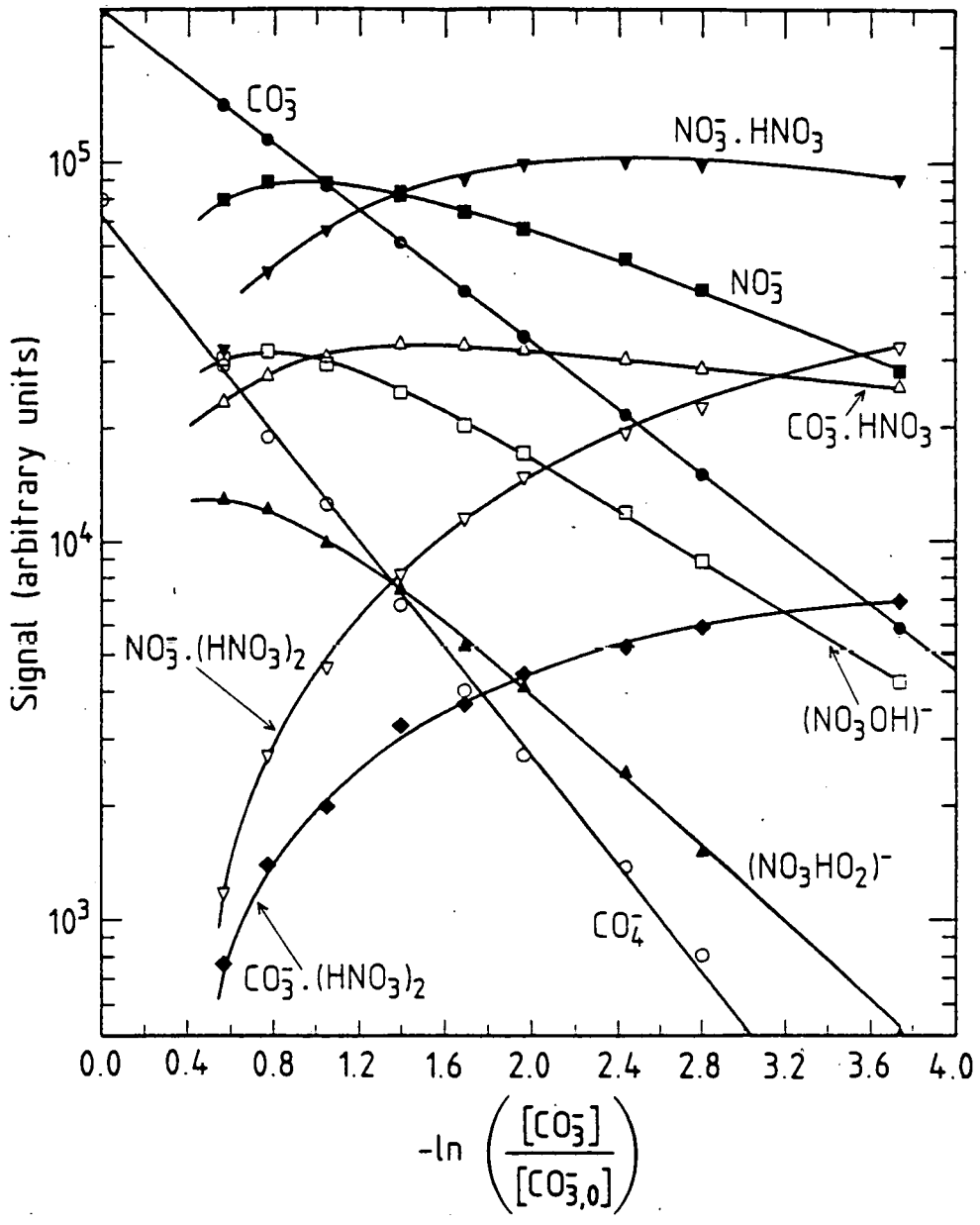

Figure 11: Count Rate of the different ions observed in figure 10c as a function of $-ln([CO_3^-]/[CO_{3,o}^-])$. A 165 sscm CO_2 flow is sent through the second ion source, along with a 200 sccm O_2-flow. A 1100 sccm Ar buffer gas flow passes through the flow tube in where the pressure equals 1.02 hPa. Upon further addition of the reactant gas, the product ions NO_3^-, $(NO_3OH)^-$ and $(NO_3HO_2)^-$ undergo secondary reactions with HNO_3 to form HNO_3–containing cluster ions.

of the $(NO_3OH)^-$ and $(NO_3HO_2)^-$ signals, which is explained by further reaction of these ions with HNO_3:

$$(NO_3OH)^- + HNO_3 \rightarrow NO_3^-.HNO_3 + OH \quad (38)$$
$$(NO_3HO_2)^- + HNO_3 \rightarrow NO_3^-.HNO_3 + HO_2 \quad (39)$$

Reaction 38 was also observed by Möhler and Arnold [7].
Relative measurements of the rate constants of reactions 37, 38 and 39 have been performed and the corresponding values are shown in table 2. Changing the source conditions allowed us to alter the relative abundance of CO_3^- and CO_4^- ions and led us to conclude that $(NO_3HO_2)^-$ is a product ion of CO_4^- with HNO_3.

4 Summary and conclusions

It was found that the poly-chloride ions Cl_2^- and Cl_3^- react rapidly with HNO_3 in the gas phase, most probably leading to the product ion $NO_3^-.HCl$. The rate coefficients for these reactions were determined relative to the reaction $Cl^- + HNO_3$ and the results are summarized in table 2. The $NO_3^-.HCl$ cluster ion is rapidly converted to $NO_3^-.HNO_3$ by further reaction with nitric acid. The latter process, and similar ones for higher order clusters, may be responsible for the low abundances of $NO_3^-.HCl$ clusters in the stratosphere.

The ion-molecule reactions of the poly-iodide ions I_2^- and I_3^- with HNO_3 were studied relative to the reaction $CO_3^- + HNO_3$ and are found to be very slow in the gas phase.

The reactions mentioned above are of peculiar interest for the described ACIMS method under development, in which the polyhalide ions are produced by the ion source.

It was also found that CO_4^- reacts rapidly with nitric acid vapour leading to NO_3^- and an ion with mass 95, identified as $(NO_3HO_2)^-$, which had not been reported previously and the structure of which is not known. The rapid reaction of CO_4^- with HNO_3 is also one of the possible pathways by which CO_4^-, which is produced in the Earth's atmosphere through reaction of CO_2 with O_2^- and $O_2^-.H_2O$, is converted to the $NO_3^-(HNO_3)_n$, clusters, which is one of the major ion families in the stratosphere.

Acknowledgments

The experiments were performed within the framework of the "MACSIMS" project, which is financed by the Commission of the European Communities within the Environment programme (contract number EV5V-CT92-0062). The authors are also indebted to the "FKFO-NFWO" (Fonds voor Kollektief Fundamenteel Onderzoek) of the Belgian National Science Foundation and to the "FKFWO-MI" (Fonds voor Kollektief Fundamenteel Wetenschappelijk Onderzoek - Ministerieel Initiatief) for partly financing this research.

Table 1

$ELECTRON\ \ AFFINITIES\ (eV)$		
M	EA	$reference$
Cl	3.617	30
Cl_2	2.4	31
NO_3	3.92	32
$BOND\ \ ENERGIES\ \ NEUTRALS\ (kcalmole^{-1})$		
$A-B$	$D(A-B)$	$reference$
$Cl-Cl$	57.2	33
$H-Cl$	103.2	30
$H-NO_3$	101.4	32
$BOND\ \ ENERGIES\ \ IONS\ (kcalmole^{-1})$		
$A^- - B$	$D(A^- - B)$	$reference$
$Cl^- - Cl_2$	17	15
$NO_3^- - HNO_3$	> 23	32
$NO_3^- - HBr$	> 21	32

Table 1: List of the thermochemical values used in this article.

Table 2

Reaction	$\frac{k_{meas}}{k_{ref}}$	k_{abs} $[10^{-10}cm^3s^{-1}]$	
		thiswork	*previous*
$Cl^- + HNO_3 \rightarrow NO_3^- + HCl$ †			16 [a]
$Cl_2^- + HNO_3 \rightarrow products$	0.30 ± 0.04	4.8	
$Cl_3^- + HNO_3 \rightarrow NO_3^-.HCl + Cl_2$	0.87 ± 0.09	13.9	
$NO_3^-.HCl + HNO_3 \rightarrow NO_3^-.HNO_3 + HCl$	0.47 ± 0.07	> 7.6	
$CO_3^- + HNO_3 \rightarrow products$ ‡			8 [a] 13 [b]
$CO_4^- + HNO_3 \rightarrow products$	1.57 ± 0.05	12.6 *	20 [b]
$O^-.HNO_3 + HNO_3 \rightarrow products$	0.85 ± 0.03	> 6.8 *	> 10 [b]
$O_2^-.HNO_3 + HNO_3 \rightarrow products$	1.11 ± 0.09	> 8.9 *	
$I^- + HNO_3 \rightarrow products$	0.018	< 0.2	< 0.5 [a]
$I_2^- + HNO_3 \rightarrow products$	0.099	< 0.8	
$I_3^- + HNO_3 \rightarrow products$	0.093	< 0.7	

Table 2: Overview of the rate constants obtained in this work and comparison with previously measured values. The rate constants derived from secondary reactions are presented as lower limits. Since I_n^- hardly reacts with HNO_3 we only present an upper limit for the corresponding rate constants.

†,‡ These reactions serve as a reference in obtaining the rate constants of all the other reactions mentioned in this table (see text).
[a] Fehsenfeld et al. (1975)
[b] Möhler and Arnold (1991)
* The discrepancy between these values and those obtained in reference b is due to the fact that for reaction ‡ the value of reference a was used to obtain absolute rate constants. Remark that this discrepancy disappears when using the value of reference b instead of a for reaction ‡.

References

[1] F. Arnold and G. Hauck, "Lower stratospheric trace gas detection using aircraft-borne active chemical ionization mass spectrometry," *Nature*, vol. 315, pp. 307–309, 1985.

[2] F. Arnold and G. Knop, "Stratospheric trace gas detection using a new balloon-borne acims method," *Int. J. Mass. Spectr. Ion Proc.*, vol. 81, pp. 33–44, 1987.

[3] H. Schlager and F. Arnold, "On stratospheric acetonitrile detection by passive chemical ionization mass spectrometry," *Planet. Space Sci.*, vol. 35, pp. 715–725, 1987.

[4] G. Knop and F. Arnold, "Nitric acid measurements in the troposphere and lower stratosphere by chemical ionisation mass spectrometry," *Planet. Space Sci.*, vol. 33, pp. 983–986, 1985.

[5] F. Arnold and G. Knop, "Stratospheric nitric acid vapour measurements in the cold arctic vortex: implications for nitric acid condensation," *Nature*, vol. 338, pp. 746–749, 1989.

[6] H. Schlager, F. Arnold, D. Hofmann, and T. Deshler, "Balloon observations of nitric acid aerosol formation in the arctic stratosphere: i. gaseous nitric acid," *Geophys. Res. Lett.*, vol. 17, pp. 1275–1278, 1990.

[7] O. Möhler and F. Arnold, "Flow reactor and triple quadrupole mass spectrometer investigations of negative ion reactions involving nitric acid: implications for atmospheric HNO_3 detection by chemical ionization mass spectrometry," *J. Atmos. Chem.*, vol. 13, pp. 33–61, 1991.

[8] D. Fussen, C. Amelynck, and E. Arijs, "Rate constant measurements for the ion/molecule reactions of $I^-, F^-, Br^- and HFBr^-$ with Cl_2," *Int. J. Mass Spect. Ion Processes*, vol. 116, pp. 13–22, 1992.

[9] F. C. Fehsenfeld, C. J. Howard, and A. L. Schmeltekopf, "Gas phase ion chemistry of HNO_3," *J. Chem. Phys*, vol. 63, pp. 2825–2841, 1975.

[10] J. A. Davidson, A. A. Viggiano, C. J. Howard, I. Dotan, F. C. Fehsenfeld, D. L. Albritton, and E. E. Ferguson, "Rate constants for the reactions of $O_2^+, NO_2^+, NO^+, H_3O^+, CO_3^+, NO_2^+$, and halide ions with N_2O_5 at 300 K.," *J. Chem. Phys.*, vol. 68, pp. 2085–2087, 1978.

[11] A. A. Viggiano, J. A. Davidson, F. C. Fehsenfeld, and E. E. Ferguson, "Rate constants for the collisional dissociation of N_2O_5 by N_2," *J. Chem. Phys.*, vol. 74, pp. 6113–6125, 1981.

[12] H. Böhringer, "Personal communication,".

[13] C. E. Melton, G. A. Ropp, and P. S. Rudolph, "Mass spectrometric observation of triatomic ions in chlorine and bromine gases.," *J. Chem. Phys.*, vol. 29, pp. 968–969, 1958.

[14] R. Robbiani and J. L. Franklin, "Formation of the trihalide ion Cl_3^- in the gas phase.," *J. Am. Chem. Soc.*, vol. 101, pp. 764–765, 1979.

[15] R. Robbiani and J. L. Franklin, "Negative ion-molecule reactions in sulfuryl halides.," *J. Am. Chem. Soc.*, vol. 101, pp. 3709–3715, 1979.

[16] L. M. Babcock and G. E. Streit, "Ion-molecule reactions of Cl_2 with Cl^- and F^-," *J. Chem. Phys.*, vol. 76, pp. 2407–2410, 1962.

[17] T. R. Hogness and R. W. Harkness, "The ionization processes of iodine interpreted by the mass spectrograph.," *Phys. Rev.*, vol. 32, pp. 785–788, 1928.

[18] G. L. Gutsev, "The structure and stability of Cl_n^- clusters, n=2-7," *Chem. Phys.*, vol. 156, pp. 427–437, 1991.

[19] E. E. Ferguson, F. C. Fehsenfeld, and A. L. Schmeltekopf, "Flowing afterglow measurements of ion-neutral reactions," *Adv. At. Mol. Phys.*, vol. 5, pp. 1–56, 1969.

[20] D. B. Dunkin, F. C. Fehsenfeld, and E. E. Ferguson, "Thermal energy rate constants for the reactions: $NO_2^- = +Cl_2 \rightarrow Cl_2^- + NO_2, Cl_2^- + NO_2 \rightarrow Cl^- + NO_2Cl, SH^- + NO_2 \rightarrow NO_2^- + SH, SH^- + Cl2 \rightarrow Cl_2^- + SH$, and $S^- + NO_2 \rightarrow NO_2^- + S$," *Chem. Phys. Lett.*, vol. 15, pp. 257–259, 1972.

[21] D. L. Christophorou, L. G.and McCorkler and C. A. A., "Electron attachment processes.," in *Electron-molecule interactions and their applications, volume 1*, (L. G. Christophorou, ed.), pp. 477–617, Academic Press, Orlando, 1984.

[22] L. C. Lee, G. P. Smith, J. T. Moseley, P. C. Cosby, and J. A. Guest, "Photodissociation and photodetachment of Cl_2^-, ClO^-, Cl_3^- and $BrCl_2^-$.," *J. Chem. Phys.*, vol. 70, pp. 3237–3246, 1979.

[23] B. M. Hughes, C. Lifshitz, and T. O. Tiernan, "Electron affinities from endothermic negative ion charge-transfer reactions. III. $NO, NO_2, SO_2, CS_2, Cl_2, Br_2, I_2$, and C_3H," *J. Chem. Phys.*, vol. 59, pp. 3162–3181, 1973.

[24] W. A. Chupka and J. Berkowitz, "Electron affinities of halogen diatomic molecules as determined by endoergic charge transfer," *J. Chem. Phys.*, vol. 55, pp. 2724–2733, 1971.

[25] R. G. Castleman, A.W.and Keesee, "Thermochemical data on gas phase ion-molecule association and clustering reactions," *J. Phys. Chem. Ref. Data*, vol. 15, pp. 1011–1071, 1986.

[26] K. Knutsen, V. M. Bierbaum, and S. R. Leone, "Thermal energy reactions of $OH^- + Cl_2, Br_2$: rate coefficients, product branching fractions and OH product vibrational populations," *Int. J. Mass Spect. Ion Processes*, vol. 119, pp. 537–555, 1992.

[27] A. A. Viggiano, "Three-body ion-molecule association rate coefficients as a function of temperature and cluster size: $NO_3^-(HNO3)_n + HCl + M \rightarrow NO_3^-(HNO3)_n(HCl) + M$," *J. Chem. Phys.*, vol. 81, pp. 2639–2645, 1984.

[28] J. L. McCrumb and F. Arnold, "High sensitivity detection of negative ions in the stratosphere," *Nature*, vol. 294, pp. 136–139, 1981.

[29] E. Arijs, D. Nevejans, P. Frederick, and J. Ingels, "Stratospheric negative ion composition measurements, ion abundances and related trace gas detection," *J. Atm. Terr. Phys.*, vol. 44, pp. 681–694, 1982.

[30] H. Hotop and W. C. Lineberger, "Binding energies in atomic negative ions. ii," *J. Phys. Chem. Ref. Data*, vol. 14, pp. 731–750, 1985.

[31] H. Dispert and K. Lacmann, "Chemiionization in alkali-halogen reactions: evidence for ion formation by alkali dimers.," *Chem. Phys. Lett.*, vol. 47, pp. 533–536, 1977.

[32] J. A. Davidson, F. C. Fehsenfeld, and C. J. Howard, "The heats of formation of NO_3^- and NO_3^- association complexes with HNO_3 and HBr.," *Int. J. Chem. Kin.*, vol. 9, pp. 19–29, 1977.

[33] R. J. LeRoy and R. B. Bernstein, "Dissociation energies of diatomic molecules from vibrational spacings of higher levels: application to the halogens," *Chem. Phys. Lett.*, vol. 5, pp. 42–44, 1970.